# Surface Alloying of Lead as a Step in the Cathodic Generation of the $Pb_9^{4-}$ in KI and RbBr Liquid Ammonia Solutions

**Jerzy B. Chlistunoff and J. J. Lagowski***

*Department of Chemistry and Biochemistry, University of Texas in Austin, Austin, Texas 78712*

*Received: November 25, 1997; In Final Form: April 8, 1998*

Reduction of lead in liquid ammonia solutions of KI and RbBr at −70 °C was studied using voltammetry as well as potentiostatic and galvanostatic techniques. It was found that the only soluble reduction product was the Zintl ion $Pb_9^{4-}$. Transitionally two intermetallic phases were also formed via direct incorporation of the alkali metal into lead, but they eventually dissolved in liquid ammonia. The alkali metal (M)-rich phase had the Pb:M molar ratio around 0.4 for both K and Rb, whereas the ratio for the lead-rich phase was between 0.8:1 and 1: 1 for potassium and around 0.7:1 for rubidium. The alkali metal-rich phase was unstable and easily transformed into the lead-rich phase by the reaction with solid lead. This reaction plays a crucial role both in the alkali metal incorporation and in the solid-phase dissolution reaction. A model mechanism of the lead reduction is presented.

## Introduction

Formation of solid phases upon the cathodic reduction of various metals and alloys in nonaqueous solvents is a quite general phenomenon.[1−11] A variety of intermetallic compounds can be produced by a direct implantation of one metal into an electrode made of some other metal.[1−10,11k,m,n,o,q,r] Solid substances are also produced upon reduction of metallic electrodes in nonaqueous solutions containing alkylammonium or ammonium salts as background electrolytes.[11b−j,l,p,s]

Among the metals that can be reduced electrochemically are those belonging to the IV and V main group of elements, which are known to form polyatomic anionic species called Zintl ions,[12] e.g., antimony,[13] bismuth,[13] tin,[14] or lead.[14] The homoatomic Zintl ions of these elements exhibit significant stability in solvents such as liquid ammonia or ethylenediamine.[12] The Zintl ions can be relatively easy produced by cathodic reduction of the respective element[15−18] or an alloy[19] in some nonaqueous solvents. Zintl ions can also be obtained by reaction of the element with an alkali metal or by dissolution of intermetallic compounds with alkali metals in certain nonaqueous solvents.[20]

In our recent paper[16] we have shown that the cathodic generation of $Pb_9^{4-}$ Zintl ions in KI solutions in liquid ammonia is accompanied by formation of solid compounds on the electrode surface. Formation of both soluble and solid products upon reduction of metallic electrodes was also observed by others.[11p,17] Such processes seem to be especially interesting, because they can provide information on the extent and mechanism of coupling between the two reduction paths. The purpose of this work is the determination of the mechanism of formation of solid compounds during the cathodic generation of $Pb_9^{4-}$ Zintl ions and their role in the reduction process. Initial studies[21] indicated no solid-phase formation using NaI and $NaClO_4$ background electrolytes. In CsI solutions, on the other hand, deposits were formed,[21] but side reactions made the processes extremely difficult to study. Therefore, our efforts are focused on KI and RbBr background electrolytes, for which reproducible results could be obtained.

## Experimental Section

A three-compartment electrochemical cell equipped with medium-porosity glass frits was used in the experiments. The electrolytes, KI Reagent, ACS (MCB, Cincinnati, OH), and RbBr (99.7%; Aldrich, Milwaukee, WI), were dried before use according to a procedure described previously.[16] The Pb disk electrodes used in this study were pretreated electrochemically before experiments by cycling at cathodic potentials, where the only reduction product is $Pb_9^{4-}$.[16] This procedure resulted in a rather rough, but reproducible, electrode surface. The same procedure could not be employed for the large electrodes used for quantitative preparative electrolyses because of the weight loss due to the electrode dissolution. Therefore, the electrodes used for preparative electrolyses were not pretreated.

All results were obtained at −70 °C with a Princeton Applied Research model 273A potentiostat controlled by an IBM-compatible computer. The potentials were measured against the silver quasi-reference electrode (AgQRE) and referenced versus the electrochemical potential of the solvated electron, which was determined according to a procedure described previously.[16] Other details of experimental procedures are described elsewhere.[16]

**Preparative Electrolyses.** A brownish-red soluble species was generated upon the reduction of a lead cathode in the entire cathodic potential window in both 0.1 M RbBr and 1.0 M KI solutions, results that are similar to those obtained previously with 0.1 M KI solutions.[16] In addition to the soluble species, gray or black deposits were also detected on the electrode surface. The stoichiometry of the soluble species was determined by its reoxidation on a Pt gauze electrode. In a typical experiment a lead electrode was reduced at a constant potential until approximately 5 C had passed through the cell. This condition corresponded to the largest charge that could be passed without the deposit flaking, a process that was manifested as a sudden increase in the reduction current. After the reduction

* Corresponding author: e-mail jjl@mail.tenet.edu; phone (512) 471-3288 (office), (512) 471-1403 (lab); fax (512) 471-8696.

S1089-5647(98)00334-4 CCC: $15.00 
Published on Web 07/03/1998

was complete, the electrode was gently lifted above the solution surface, and the solution was reoxidized on a Pt gauze electrode at 1.2−1.3 V vs solvated electron potential until approximately 1 C passed. The Pt electrode was then gently removed from the solution and dried, and the deposited lead was dissolved in a 1:5 nitric acid. The resulting acidic lead nitrate solution was diluted to a known volume and analyzed using inductively coupled plasma (ICP) spectroscopy. The number of electrons ($n$) associated with a single Pb atom in the anionic species ($Pb^{n-}$) was calculated from the oxidation charge and mass of the Pb deposit. The $n$ value was independent of the cathodic generation potential and equal to 0.452 and 0.448 for 0.1 M RbBr and 1.0 M KI, respectively. These values are very similar to those obtained for 0.1 M KI solutions[16] and suggested that the soluble species generated is $Pb_9^{4-}$. That the substance generated is $Pb_9^{4-}$ was confirmed by voltammetry, which exhibited a single, irreversible oxidation peak with the current controlled by diffusion for both electrolytes studied.

The deposits formed upon the lead reduction would not dissolve in pure liquid ammonia. However, they were moderately unstable in air and dissolved violently in a diluted (1:5) nitric acid. The end of dissolution, which usually occurred in a fraction of a second, was manifested by almost complete disappearance of the hydrogen evolution and a shiny look of the electrode. The deposits are believed to be intermetallic compounds of lead and the alkali metals. Their stoichiometry was estimated from the electrolysis charge and the electrode weight losses before and after dissolution of the deposit, assuming that the only soluble species produced was $Pb_9^{4-}$. The electrodes were thoroughly washed with either liquid ammonia or anhydrous methanol before weighing. Any contact with the air during washing was avoided by using a combination of Schlenk line and drybox techniques. The weight measurements (in air) were performed immediately after removing the electrode from the water/air-free atmosphere (gaseous ammonia or helium) to minimize errors associated with partial oxidation of the deposit in air. However, we note that even if partial oxidation occurred, the expected error resulting from it was relatively small, because of the relatively low atomic weight of oxygen (16) when compared to lead (207.2).

The molar ratio of lead to rubidium in the lead rubidium compound was ranging between 1.9:1 and 4.5:1 (average 2.9) with some tendency to increase with time (0.5−2 h) that passed between the end of electrolysis and weighing, which suggested occurrence of a chemical reaction involving the initially formed deposit and lead. For 1.0 M KI solutions only two qualitative experiments were performed at the single potential 0.27 V. The average Pb:K molar ratio obtained was 1.96:1. The ratios given above remain in the range of composition of known lead/rubidium and lead/potassium compounds.

Prolonged electrolysis frequently resulted in separation of the initially formed deposit from the lead surface. If the electrolysis was then continued, only a small amount of the deposit could be produced. In addition, when the electrode with the deposit was lifted over the solution surface (gaseous ammonia atmosphere), the deposit disappeared within several seconds, leaving a shiny metal surface behind. When the electrode after the deposit disappearance was treated with a diluted nitric acid, no vigorous bubbling typical of a lead−alkali metal compound was observed. This effect suggested that the deposit simply dissolved in the thin layer of ammonia that was left on the electrode surface. The detailed studies, described below, fully support that hypothesis.

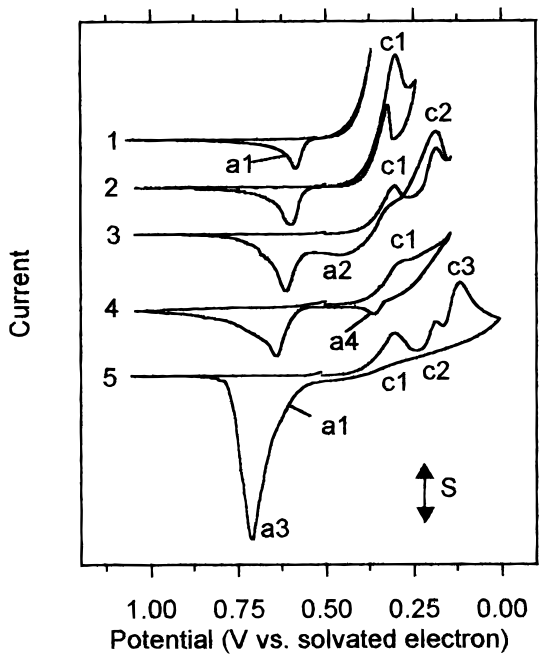


**Figure 1.** Voltammograms of a 1 mm Pb disk in 0.1 M RbBr at −70 °C. Scan rate: 50 mV/s (1−3, 5), 0.5 V/s (4). *S*: 25 $\mu$A (1), 50 $\mu$A (2), 125 $\mu$A (3), 250 $\mu$A (4, 5).

The effect of increased stability of the deposits formed on electrodes, which were not pretreated electrochemically,[16] requires a separate study. It seems, however, that these deposits are most likely due to the presence of a thin layer of a lead carbonate/oxide on the untreated electrodes. This layer, if it is not destroyed during early stages of the reduction, can inhibit the lead dissolution process and leads to the accumulation of solid phases on the surface. Once the protective layer is destroyed, the lead dissolution occurs much faster.

**Cyclic Voltammetry.** Cyclic voltammograms of a lead disk in 0.1 M RbBr (Figure 1) are similar to the voltammograms recorded for 0.1 and 1.0 M potassium iodide solutions.[16] The reduction currents measured at relatively low cathodic potentials ($E$ > 0.33 V) increase approximately exponentially with the cathodic overpotential and are virtually independent of the scan rate (20 mV/s−20 V/s) as expected for a totally irreversible reaction. Only a single irreversible oxidation peak a1 is associated with the reduction performed under such conditions. Similarly to the results obtained with KI solutions,[16] this peak is attributed to the oxidation of $Pb_9^{4-}$. When the cathodic potential limit was extended to 0.24 V at a scan rate 50 mV/s, a cathodic peak, labeled c1, appeared on the voltammogram. A similar cathodic peak could also be observed on the anodic scan (Figure 1). No new reduction products associated with the peak c1 could be detected. The anodic peak a1 was then, however, slightly distorted. Further extension of the cathodic potential limit resulted in formation of another cathodic peak, labeled c2 (Figure 1). This peak was also accompanied by a similar cathodic peak in the anodic scan, but the currents measured in the anodic scan were higher. Similar hysteresis effects were also observed for KI solutions.[16] With the peak c2 at low scan rates (e.g., 50 mV/s) there was also associated a broad anodic peak at a potential around 0.45 V; this peak is labeled a2. An analogous peak was previously detected for KI solutions.[16] When higher scan rates (e.g., 0.5 V/s or higher) were used, the peak c1 still existed but the anodic peak a2 disappeared. Instead, another anodic peak, labeled a4 (Figure 1), formed at less cathodic potentials (Epa = 0.36 V at $\upsilon$ = 0.5 V/s). An

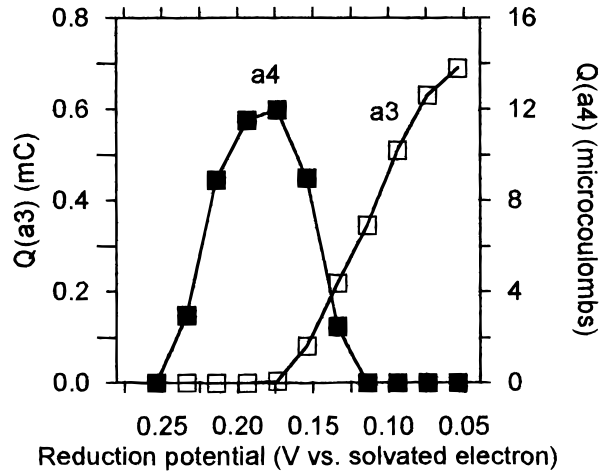


**Figure 2.** Electrical charges of peaks a3 and a4 (see text) plotted versus the reduction potential. Reduction time 5 s. Anodic scan rate 5 V/s.

analogous peak was also detected for KI electrolytes.[16] Further extension of the cathodic potential limit to 0 V at high scan rates produced no remarkable changes in the voltammogram. At low scan rates, however, a new cathodic peak, labeled c3, could be seen on the voltammogram as well as a corresponding large anodic peak (a3) centered around 0.7 V, which overlapped with the oxidation peak of $Pb_9^{4-}$ (Figure 1). A peak similar to a3 was also found for KI solutions[16] and attributed to oxidation of a K/Pb intermetallic compound.

We must point out that the two peaks observed in the voltammograms using KI solutions, which are analogous to the peaks a2 and a3, were labeled differently in the previous study.[16] The large anodic peak, centered around 0.7 V, here denoted as a3, was labeled a2 in the previous paper,[16] and vice versa. It seems that the current labeling is more logical, and therefore, this labeling procedure will is used throughout this paper for both RbBr and KI solutions.

The anodic peaks a2, a3, and a4 in both RbBr and KI electrolytes exhibited properties typical of surface confined species as indicated either by the peak shape (a3 and a4) or by the lack of influence of solution stirring on the oxidation current (a2, a3, and a4). There was no effect of stirring on the reduction currents either, which suggests that the surface confined species s2, s3, and s4, corresponding to the oxidation peaks a2, a3, and a4, are not formed by precipitation of some soluble anionic species with the alkali metal cations.

The charges associated with the peaks a2 and a3 were usually on the order of millicoulombs, whereas the charges obtained for the peak a4 were typically on the order of microcoulombs. In addition, for both 1.0 M KI and 0.1 M RbBr electrolytes, the charge associated with a4 seemed to tend to a limiting value of approximately 14 $\mu$C (approximately 1800 $\mu$C/cm$^2$) when either the scan rate or the cathodic reversal potential was increased, provided there was no other oxidation peaks beyond a4 and a1 (Figure 1). The presence of other anodic peaks was always associated with a decrease in the a4 charge. For instance, a negative correlation was detected between the charge of a4 and that of a3, corresponding to oxidation of the lead−potassium intermetallic compound[16] in 1.0 M KI solutions (Figure 2).

Our observations suggest that the peaks a2 and a3 represent the oxidation of intermetallic compounds of lead and the alkali metal. As will be shown in the next section, potentiostatic and galvanostatic experiments support that conclusion. The peak a4, on the other hand, most likely represents oxidation of the underpotential deposited[22,23] alkali metal. Its high charge density of 1800 $\mu$C/cm$^2$ would correspond to a monolayer of potassium or rubidium if the roughness factor of the electrode, i.e., ratio of its real to geometrical surface area, was around 18. Even though such a high number seems reasonable for our nonpolished and electrochemically activated,[16] i.e., strongly corroded, electrodes, the possibility of a multilayer deposition[11q,24,25] cannot be excluded either. That the peak a4 is detected at high scan rates only is most likely associated with the fact that the electrode dissolves upon reduction, and this reaction can effectively remove the adsorbed alkali metal from the surface. More detailed studies[26] of this effect prove the correctness of such an interpretation. Similarly, the finding that the oxidation peak a4 disappears when a layer of a intermetallic compound is formed remains in agreement with this interpretation.

**Potentiostatic Method.** At the potentials where only $Pb_9^{4-}$ was produced in KI or RbBr solutions (see above), the chronoamperometric $i-t$ transients exhibit an initial current decay, which is followed by a steady-state current (Figure 3). More negative reduction potentials result in the occurrence of current peaks that follow the initial current decay. At shorter times and/or lower cathodic potentials a single peak is observed for 1.0 M KI solutions, whereas one or two relatively closely spaced peaks are observed for 0.1 M RbBr solutions (Figure 3a,b) under similar conditions. The time at which the peak(s) occurred decreased on increasing the cathodic overvoltage (Figure 3).

If the potentiostatic reduction was stopped right after the first peak was formed in 0.1 M RbBr solution (see curve 2, Figure 3a), and it was immediately followed by an anodic voltammetric scan (50 mV/s), the oxidation peak a2 (Figure 1) could be detected. This peak, however, is usually accompanied by a small peak a3. For 1.0 M KI solution the oxidation peak a2 can only be observed when the potentiostatic reduction is stopped during increasing portion of the first reduction peak and when higher anodic scan rates, e.g., 0.2 V/s, are used. When the reduction is stopped after a single peak is formed in 1.0 M KI solution (curve 2, Figure 3b) or the second peak is formed in 0.1 M RbBr solutions (curves 3−6, Figure 3a), only the presence of the deposit s3 (oxidation peak a3, Figure 1) is detected on the electrode surface. Higher reduction potentials and/or significantly longer reduction times did not result in formation of new reduction products, even though new cathodic peaks were observed on the $i-t$ transients (Figure 3b, curves 3 and 4). The only surface product detected was the deposit s3 for both 0.1 M RbBr and 1.0 M KI electrolyte.

The above results suggest that the species s2, which is formed at relatively shorter reduction times, can be transformed into s3 when the electrolysis progresses. The current peak, which is formed after extremely long electrolysis (Figure 3b, curves 3 and 4), is not very well defined and most likely results from some structural changes occurring to the electrode surface, e.g., the significant expansion[27−29] of the deposit resulting from high molar volumes of the incorporated metals. An increase in the electrode surface area due to the deposit cracking[30] seems also possible as manifested by irregularities on transients recorded for high cathodic overvoltages (curve 4, Figure 3b).

Transients similar to those shown in Figure 3a,b were reported in the literature for other metallic electrodes undergoing cathodic reduction in nonaqueous media in the presence of salts of other metals[6−8,11o] where the reduction leads to formation of intermetallic compounds. An initial current decay is usually interpreted in terms of formation of solid solution,[6,7,11o] the rate of which is frequently governed by the diffusion[1,3,4,7,10,30] of

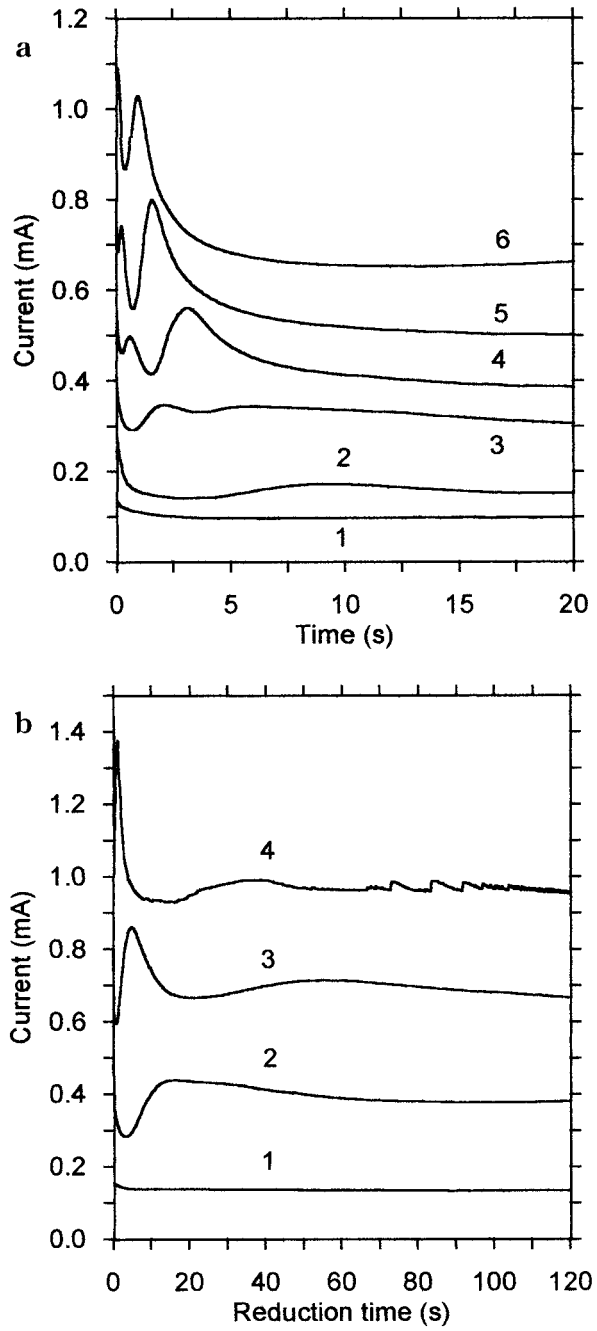


**Figure 3.** (a) Potentiostatic $i-t$ transients recorded for a 1 mm Pb disk in 0.1 M RbBr solution at − 70 °C. Reduction potentials (V): 0.325 (1), 0.275 (2), 0.225 (3), 0.175 (4), 0.125 (5), 0.025 (6). For clarity the curves 2−6 shifted toward higher currents by 0.1, 0.2, 0.3, 0.4, and 0.5 mA, respectively. (b) Potentiostatic $i-t$ transients recorded for a 1 mm Pb disk in 1.0 M KI solution at − 70 °C. Reduction potentials (V): 0.374 (1), 0.324 (2), 0.274 (3), 0.224 (4). For clarity the curves 2−4 shifted toward higher currents by 0.2, 0.4, and 0.6 mA, respectively.

the metal being incorporated in the solid matrix. This process is followed by crystallization of an intermetallic phase, which leads to a current increase.[6−8,11o]

In the present case no oxidation peak on the voltammograms could be attributed to oxidation of a solid solution of K or Rb in Pb. The peaks a1, a3, and a4 are due to the oxidation of $Pb_9^{4-}$, an intermetallic compound, and the underpotential deposited alkali metal, respectively. The charges associated with the peak a2 seem too high for oxidation of presumably diluted[2,5] solid solution of the alkali metal in lead (see the section on the deposit stoichiometry determination). It seems then possible that the (presumably) diffusion-controlled oxidation peak of the solid solution of K or Rb in Pb can be masked by the significantly larger oxidation peak of $Pb_9^{4-}$. As noted above, the oxidation peak of $Pb_9^{4-}$ (a1) was slightly distorted when the cathodic reversal potential was lower than the c1 peak potential (see Figure 1). Note also that the dissolution of the electrode ($Pb_9^{4-}$ generation) can effectively remove the alkali metal that was incorporated, thus making its detection even more difficult. Therefore, the initial, relatively slow current decay (Figure 3a) cannot be attributed to formation of the solid solution of the alkali metal in Pb, even though such a reaction most likely takes place. More detailed studies of processes occurring during the very initial stages of the cathodic reduction of Pb or at potentials where only $Pb_9^{4-}$ is generated are underway. These studies[26] strongly suggest that the initial current decay results mainly from surface reactions of the underpotential deposited alkali metal.

The first and second current maxima on the $i-t$ transients originate from formation of new crystalline compounds (s2 and s3). The current increase associated with the formation of the first solid phase (s2) in 0.1 M RbBr (Figure 3a) solution is easily understood. When the compound s2 starts being formed, the local activity of the alkali metal on the surface and in the solid solution significantly decreases, which creates a driving force for further alkali metal deposition/incorporation and leads to the current increase. The driving force also depends on the reduction potential, since the equilibrium activity of the alkali metal increases with the cathodic overpotential according to the Nernst equation. Therefore, the current increases more rapidly, and current maxima are formed after shorter reduction times at more cathodic reduction potentials. As the electrolysis progresses, the zones, in which the new phase is formed, expand,[31] and the diffusion field for the alkali metal gradually becomes smaller, which eventually leads to the observed current decrease. The subsequent current increase (foot of the second peak in 0.1 M RbBr solution) suggests that more rubidium can be incorporated in lead. One can, therefore, suspect that a compound with higher content of Rb is formed. The actual stoichiometry determinations (see below) reveal, however, that the second compound formed (s3) actually contains relatively smaller amounts of rubidium. Thus, a mechanism involving an enhanced intake of rubidium does not seem completely clear. Most likely the process is associated with structural changes occurring in the deposit layer upon reduction and/or higher thermodynamic stability of the lead-rich phase s3. For KI electrolyte (Figure 3b) both phases seem to form simultaneously, or s2 is rapidly converted into s3.

Once the deposit s2 is completely converted into s3 and the s3 forms a uniform, compact layer on the electrode surface, further growth is possible only when the alkali metal can reach deeper layers of lead. The rate of such processes can be controlled either by the rate of diffusion of the alkali metal atoms and possibly lead atoms through the compound s3 layer or by the rate of the compound formation.[32] In each case a different type of the current versus time behavior is expected. According to the literature a steady-state current results from kinetic control,[32] whereas linear $i$ vs $1/t^{1/2}$ dependence[32] indicates diffusion control. Strictly linear $i$ vs $t^{-1/2}$ dependence would be expected for a diffusion-controlled process if the deposit was present on the electrode surface from the very beginning of the electrolysis, whereas some part of the electrical charge is consumed for the formation of the compact layer during the initial period of the electrolysis. In such cases a linear dependence of current versus $(t - t_0)^{1/2}$ would be expected,

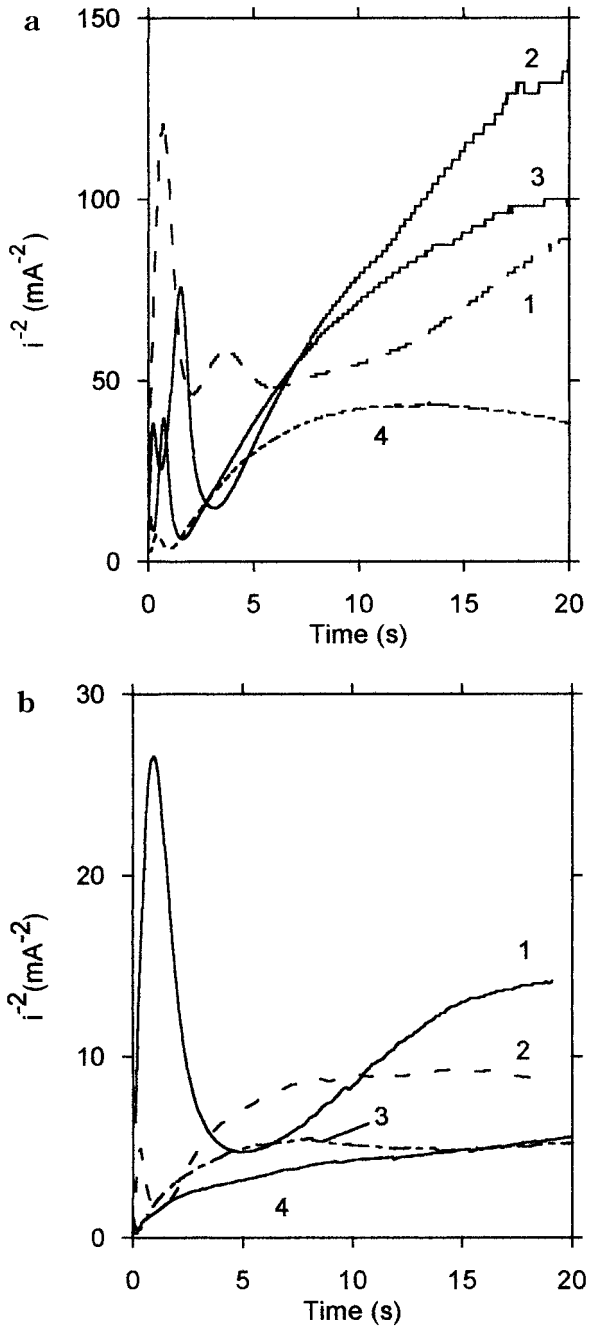


**Figure 4.** (a) Potentiostatic $i-t$ transients recorded for a 1 mm Pb disk in 0.1 M RbBr solution at − 70 °C plotted in $1/i^2$ vs $t$ coordinates (see text). Reduction potential (V): 0.225 V (1), 0.175 V (2), 0.125 V (3), 0.025 V (4). (b) Potentiostatic $i-t$ transients recorded for a 1 mm Pb disk in 1.0 M KI solution at − 70 °C plotted in $1/i^2$ vs $t$ coordinates (see text). Reduction potential (V): 0.274 V (1), 0.224 V (2), 0.174 V (3), 0.124 V (4).

where $t_0$ represents the time passed for the formation of the compact layer. Because the moment when the compact layer is formed ($t_0$) cannot be determined precisely from the $i-t$ transients, we plot $1/i^2$ vs time, since this method is free of such an ambiguity.

Figure 4 shows the $1/i^2$ plots obtained for 0.1 M RbBr and 1.0 M KI solutions at different reduction potentials. As can be seen, the rate-determining step for the reduction on an electrode covered with the deposit could not be determined unequivocally. Some approximately linear sections can be observed on $1/i^2$ vs $t$ plots at relatively short times after the maximal current is reached (minimum of $1/i^2$), but at longer electrolysis times the slopes of those lines decrease (Figure 4). This tendency does not indicate a change from the diffusion to kinetic control (steady state) of the reaction, since the rate of diffusion decreases with the electrolysis time. Formation of the additional current peak is responsible for the observed behavior (Figure 3b, curves 3 and 4). As mentioned above, no new reduction products are associated with this peak.

In principle, the approximately linear sections of plots shown in Figure 4 could be used for the determination of the alkali metal diffusion coefficient in the intermetallic compound s3.[8,27−29,33,34] However, the concentration gradient of the alkali metal in the compound layer is not known, and therefore, the diffusion coefficient cannot be determined without oversimplifying assumptions. A quantitative analysis would be additionally complicated by the fact that formation of the intermetallic compound is not the only process occurring during the cathodic polarization of lead. Formation of $Pb_9^{4-}$, which occurs at a different rate, contributes to the measured current as well.

The contribution of the $Pb_9^{4-}$ formation to the total reduction current cannot be measured by a simple integration of the anodic voltammetric peaks corresponding to oxidation of $Pb_9^{4-}$ and s3 (Figure 1), because part of the $Pb_9^{4-}$ diffuses away during the reduction. In the method that was used for 0.1 M RbBr solutions, we coupled double potential step chronoamperometry with intensive stirring of the solution. In the first step, lead was reduced at a potential where both the deposit s3 and $Pb_9^{4-}$ were formed. At the potential of the second step (1.37 V) both products could be oxidized. However, vigorous stirring transported $Pb_9^{4-}$ away from the electrode surface. In this way the substance oxidized in the second step was almost exclusively the solid compound s3. In consequence, the difference of the cathodic and anodic charges corresponded to the charge that was consumed for the generation of $Pb_9^{4-}$. The relative contribution of $Pb_9^{4-}$ in the total charge due to the reduction was found to decrease with cathodic overpotential. However, the absolute contribution associated with this process increased weakly with the reduction potential from approximately 25 mA/cm$^2$ at 0.19 V to around 32 mA/cm$^2$ at 0.09 V (Figure 5). Such a weak potential dependence of the rate of $Pb_9^{4-}$ formation suggests occurrence of chemical, i.e., potential independent, reactions coupled to the charge-transfer reaction. An increased contribution from $Pb_9^{4-}$ was observed at less cathodic overpotentials (curves 2 and 3, Figure 5) where probably part of the electrode surface is not covered with the deposit and the direct $Pb_9^{4-}$ generation can occur as well.

**Galvanostatic Method.** A flat potential response typical of noncomplicated, completely irreversible electrode reaction is observed for RbBr and KI electrolytes at low reduction current densities when no solid compound is formed. On the other hand, a potential minimum (or minima) could be observed in the $E-t$ transients recorded for sufficiently high current densities, which resulted in the deposit formation (Figure 6). Similar to the results of potentiostatic studies (see above), the behavior (minima in the $E-t$ transients) seems to be a manifestation of an electrocrystallization process. The application of a current pulse shifts the electrode potential from its open circuit value to the value characteristic for the very first reaction that can occur with a rate determined by the applied current. At sufficiently high current densities, incorporation of the alkali metal into lead and formation of the new phase occurs. This reaction, however, cannot occur until stable product nuclei are formed, a process which requires some additional overvoltage. Therefore, in the initial stage the electrode potential is shifted

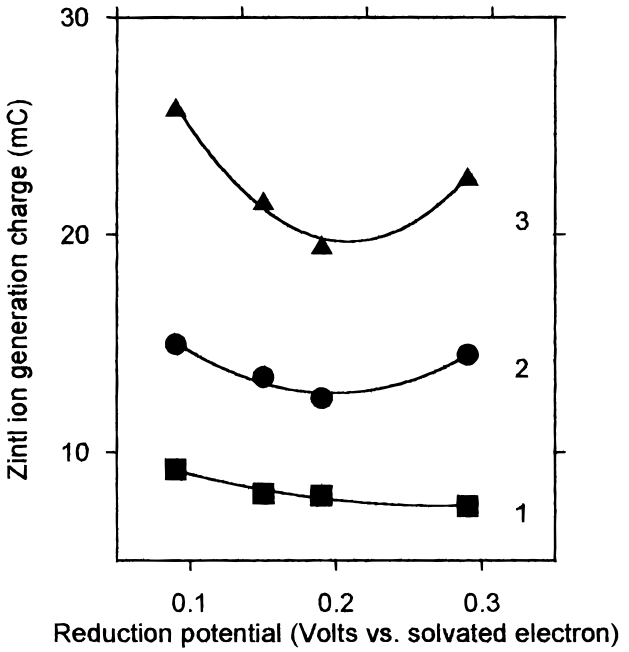


**Figure 5.** Zintl ion generation charge in 0.1 M RbBr solution at − 70 °C at a 1 mm Pb disk obtained from double potential step chronoamperometry (see text). Reduction time (s): 40 (1), 60 (2), 100 (3).

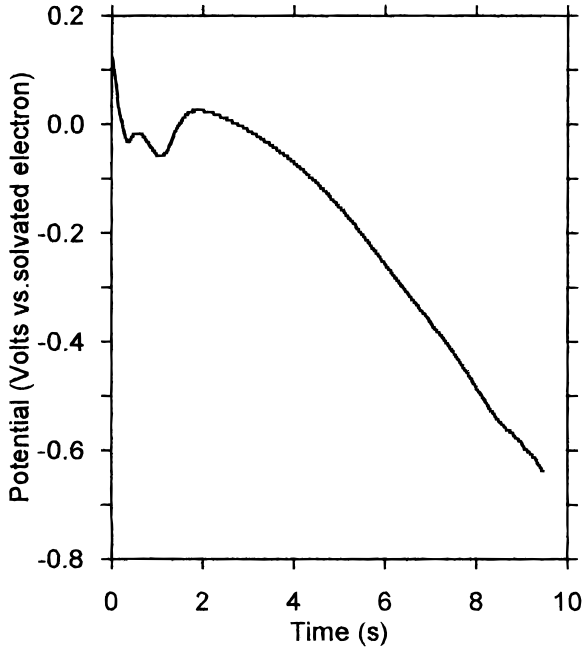


**Figure 6.** Galvanostatic $E-t$ transient obtained for a 1 mm Pb disk in 0.1 M RbBr solution at − 70 °C. Reduction current 220 $\mu$A.

significantly in the cathodic direction. Once product nuclei are formed, crystals of the new phase can grow at a relatively lower cathodic potential, resulting in the potential minimum that is observed. However, the growth of the crystalline phase inhibits the transport of the alkali metal to the deeper layers of lead. Therefore, the potential eventually starts shifting in the cathodic direction again to maintain the specific rate of the incorporation which is determined by the applied current.

The electrical charges corresponding to the potential minimum or to a subsequent potential minimum (Figure 6) decreased with the reduction current, as would be expected from the simultaneous formation of $Pb_9^{4-}$.

**Rest Potential of the Lead Electrode.** Irrespective of the technique applied, the rest potential of the electrode after

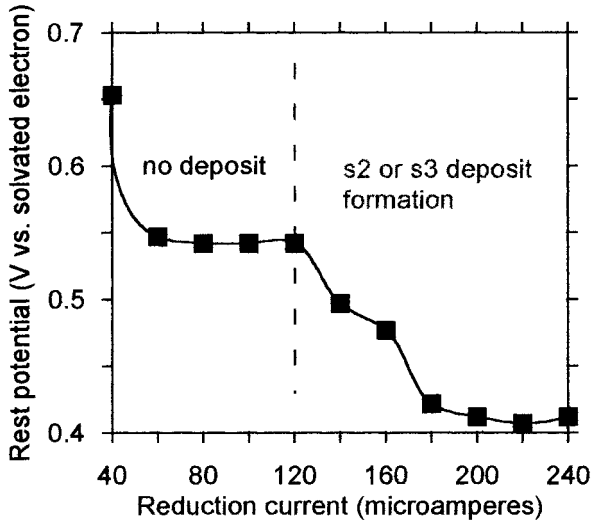


**Figure 7.** Effect of the reduction current on the rest potential of a 1 mm Pb disk measured after 10 s galvanostatic reduction in 0.1 M RbBr at − 70 °C.

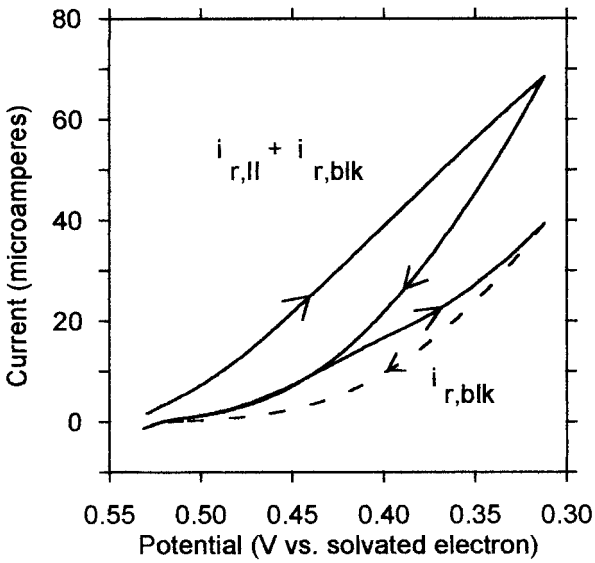


**Figure 8.** Two subsequent cathodic scans recorded for a 1 mm Pb disk covered with porous lead II (see text). Scan rate 50 mV/s.

reduction was close to the $Pb_9^{4-}$ oxidation potential in those cases when no deposit was formed. Formation of either s2 or s3 shifted the rest potential cathodically close to the a2 (s2 oxidation) peak potential (Figure 7) in both KI and RbBr electrolytes.

**Stoichiometry of the Intermetallic Deposits Formed on Activated Lead Electrodes.** The method we used in determining the stoichiometry of the Pb/K and Pb/Rb phases is similar to the stripping method applied recently for zinc/nickel alloys.[35] As found previously,[16] the lead that is formed upon oxidation of a solid compound s3 is either very fine crystalline or amorphous solid (further referred to as lead II) that can be dissolved easily by cathodic reduction to $Pb_9^{4-}$ at the potentials where no deposit formation takes place (Figure 8). The number of moles $n_{PbII}$ of lead II is proportional to its reduction charge $Q_{r,II}$ at the potentials where only Pb dissolution occurs:

$$n_{PbII} = (9/4)Q_{r,II}/F \quad (1)$$

where the factor 9/4 results from stoichiometry of the lead dissolution reaction

$$9\mathrm{Pb} + 4\mathrm{e}^- \rightleftharpoons \mathrm{Pb}_9^{4-} \quad (2)$$

The number of moles $n_M$ of the alkali metal M in the deposit (s2 or s3), on the other hand, is proportional to the charge ($Q_{ox,dep}$) associated with the oxidation of the deposit ($Pb_xM_y$)

$$n_M = Q_{ox,dep}/F \quad (3)$$

because removal of one alkali metal atom from the deposit is associated with a transfer of one electron:

$$\mathrm{Pb}_x\mathrm{M}_y \rightleftharpoons x\mathrm{Pb} + y\mathrm{M}^+ + y\mathrm{e}^- \quad (4)$$

Consequently

$$Q_{r,II}/Q_{ox,dep} = 4n_{Pb}/9n_M = 4x/9y \quad (5)$$

where the $x/y$ ratio represents the molar ratio of lead and alkali metal in the deposit.

While the determination of $Q_{ox,dep}$ is a straightforward procedure based upon integration of the oxidation peak of the intermetallic compound, $Q_{r,II}$ cannot be obtained in an identical way because lead II and bulk lead are reduced at the same potential[16] (see Figure 8). The total reduction current at the potentials where only $Pb_9^{4-}$ is formed is always a sum of contributions resulting from reductions of both the lead II ($i_{r,II}$) and the bulk lead ($i_{r,blk}$):

$$i_{tot} = i_{r,II} + i_{r,blk} \quad (6)$$

The two contributions in eq 6 are interrelated. For very thick lead II films, $i_{r,blk}$ can approach zero, since only lead II will be reduced. For thin and very porous films, $i_{r,blk}$ can be equal to the lead reduction current in the absence of any deposit. Since there is no obvious way to estimate the exact contribution of both forms of lead in the total reduction current, we made an assumption that $i_{r,blk}$ is equal to the bulk lead reduction current in the absence of any deposit. This assumption will always lead to the underestimated $i_{r,II}$ (see eq 6) and $x/y$ (eq 5), but this effect is likely to be small. For very thick layers of lead II $i_{r,II}$ would significantly exceed $i_{r,blk}$. Therefore, even if $i_{r,blk}$ was significantly diminished by the presence of lead II, the determination of $i_{r,II}$ would not be affected remarkably. For thinner lead II films the $i_{r,blk}$ is most likely relatively less affected by the presence of Pb II.

The procedure used to determine the amount of lead II, which was produced upon oxidation of the intermetallic phases, depended on the voltammetric reduction at a scan rate of 50 mV/s in the potential range where only the reaction 2 occurred. The cathodic scan was extended as far as possible into cathodic region in order to reduce number of scans necessary to dissolve Pb II completely. The current recorded for each scan was corrected for $i_{r,blk}$ (eq 6) measured in the absence of any deposit and integrated. The charges from subsequent scans were added. We assumed that the complete dissolution of Pb II occurred when the current measured in the last scan did not exceed $i_{r,blk}$ by more than 2%. The systematic error resulting from incomplete dissolution of lead II was expected to be much lower than 2% for thick Pb II films and at most 2% for the thinnest films studied.

The influence of a variety of factors on the determination of the stoichiometry of the deposits generated cathodically was investigated. These studies were mainly focused on deposit s3, which is formed in large quantities. Among the factors studied were generation time in a potentiostatic and galvanostatic regime, generation potential and current, scan rate for the deposit oxidation reaction, generation mode, and the delay time at an open circuit potential between the cathodic generation and the deposit oxidation.

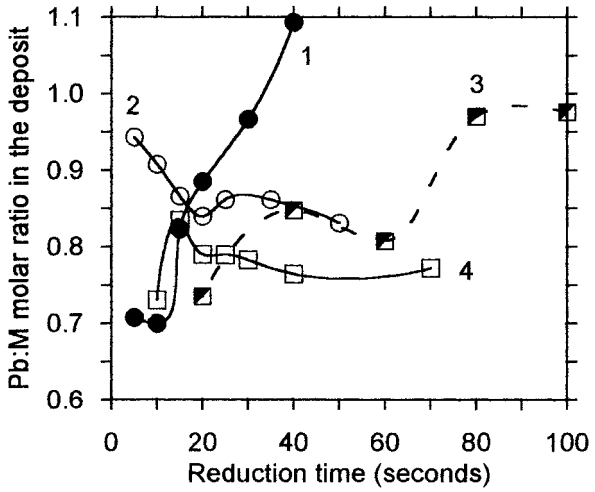


**Figure 9.** Effect of the reduction time on the apparent stoichiometry of the s3 deposit (see text) when the voltammetric oxidation immediately followed potentiostatic reduction. Scan rate 50 mV/s. Electrolyte: 0.1 M RbBr (1, 3), 1.0 M KI (2), 0.1 M KI (4). Reduction potential (V): 0.028 (4), 0.12 (1), 0.17 (3), 0.27 (2).

In the first series of experiments a lead disk electrode was reduced at a constant potential for a specified time, and then the potential was immediately scanned anodically to oxidize the reduction products. Although generally different behavior was observed for KI and RbBr electrolytes, the influence of the scan rate and the reduction time on the stoichiometry of s3 was too difficult to explain by any simple model. For instance, a small decrease of Pb:K ratio on increasing the reduction time was observed for 0.1 and 1.0 M KI electrolytes, whereas an increase of Pb:Rb was found for 0.1 M RbBr from similar experiments (Figure 9). In general, the molar ratio of lead to the alkali metal was found to vary between around 0.65:1 and 1.1:1. The reduction potential, on the other hand, was found to have no remarkable effect on the Pb:M molar ratio in the s3 deposit. Irrespective of the reduction potential, the Pb:K ratio measured for 1.0 M KI solution was generally higher (around 0.9) than the Pb:Rb ratio measured for 0.1 M RbBr solution (around 0.7).

Since both the scan rate and the reduction time were found to affect the stoichiometry (see above), indicating the importance of some kinetic factors, a series of experiments were designed to minimize these effects. After the deposit was generated for a specified time, the potentiostat was disconnected and the electrode equilibrated for a specified time at the open circuit potential. The shortest equilibration time was 30 s. Then the anodic voltammogram was recorded at a single low scan rate of 50 mV/s. As was expected, neither the reduction time nor the equilibration (delay) time (700 s $> t_d >$ 30 s) nor the reduction potential was found to have a significant influence on the Pb:M ratio under such conditions. The amount of the deposit, however, was found to decrease with the delay time (see section below). The generation mode, i.e., potentiostatic or galvanostatic, did not influence the s3 stoichiometry either. The ratio, however, depended on the electrolyte used, being highest ($0.975 \pm 0.055$, the average from 29 experiments) for 1.0 M KI, lower for 0.1 M KI ($0.780 \pm 0.060$, the average from 32 experiments), and the lowest for 0.1 M RbBr ($0.661 \pm 0.039$, average from 21 experiments).

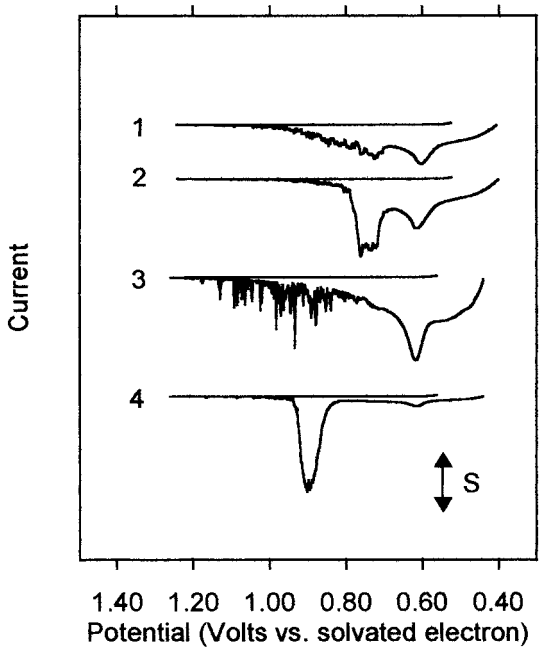


**Figure 10.** Anodic voltammograms recorded for a 1 mm Pb disk in 0.1 M RbBr (1, 2) and 1.0 M KI (3, 4) after 10 s of a galvanostatic reduction. Reduction currents (mA): 0.2 (1), 0.22 (2), 0.60 (3), 0.70 (4). Delay time (s): 30 (1), 32 (3), 34 (2), 45 (4). $S = 50\ \mu$A (1−3) and 500 $\mu$A (4).

A similar technique was used to determine the stoichiometry of the s2 deposit. In this case, however, a combination of a galvanostatic reduction (see above) and voltammetry gave the most reliable results. We found that some combinations of the reduction time, current, and the delay time between the reduction and the oxidation resulted in anodic voltammograms, in which the anodic peak s2 was predominant (Figure 10). We found that the species s2, which gives rise to the peak a2, has a composition corresponding to the lead:alkali molar ratio around 0.42:1 for 1.0 M KI and around 0.39:1 for 0.1 M RbBr. Although these numbers may be less accurate than these for the s3 deposit, there is no doubt that the s2 deposit contains relatively more alkali metal than the s3.

**Dissolution of the Intermetallic Deposits.** As was expected, the deposit s3 was found to dissolve in liquid ammonia, which was manifested by a decrease of the deposit oxidation charge on increasing the delay time between the potentiostatic reduction and the deposit oxidation. Typical anodic voltammograms recorded after different equilibration times for 1.0 M KI solution are shown in Figure 11. As could be seen from Figure 11, the decrease of the deposit oxidation charge is also accompanied by narrowing of the oxidation peak (a3); its anodic shift suggests progressive stabilization of the deposit, most likely due to the recrystallization process. Similar anodic shifts of the peak a3 were also observed for RbBr, although in that case the effect was not as strong. A small decrease of the s3 dissolution rate with time (Figure 12) may also reflect the same phenomenon. The initial rate of dissolution was 0.96, 3.1, and 2.0 mA/cm$^2$ for 1.0 M KI, 0.1 M KI, and 0.1 M RbBr, respectively, as measured by the oxidation charge of the deposit. These numbers are about 1 order of magnitude lower than the rates of $Pb_9^{4-}$ generation at the highest cathodic overpotentials applied (see Figure 5), suggesting that the process producing $Pb_9^{4-}$ is predominantly electrochemical in nature, even though some chemical reactions contribute to the overall reaction.

An important observation associated with dissolution of the deposits was that peak a1 was always present in the voltammograms recorded after different equilibration times. This observation suggests that $Pb_9^{4-}$ is a dissolution product, since any $Pb_9^{4-}$ formed as a primary reduction product would have diffused away. In many cases the peak a1 was, however, distorted (Figure 11), especially for thick deposit layers. Such distorted peaks were found to be virtually insensitive to stirring. Therefore, we believe that the distorted peak a1 resulted from oxidation of $Pb_9^{4-}$ entrapped in the deposit pores. After sufficiently long time complete dissolution of the deposit occurs. Cathodic reduction of the electrode after the deposit dissolution revealed no presence of porous lead II, since the reduction currents were identical to those recorded for the freshly activated electrode.

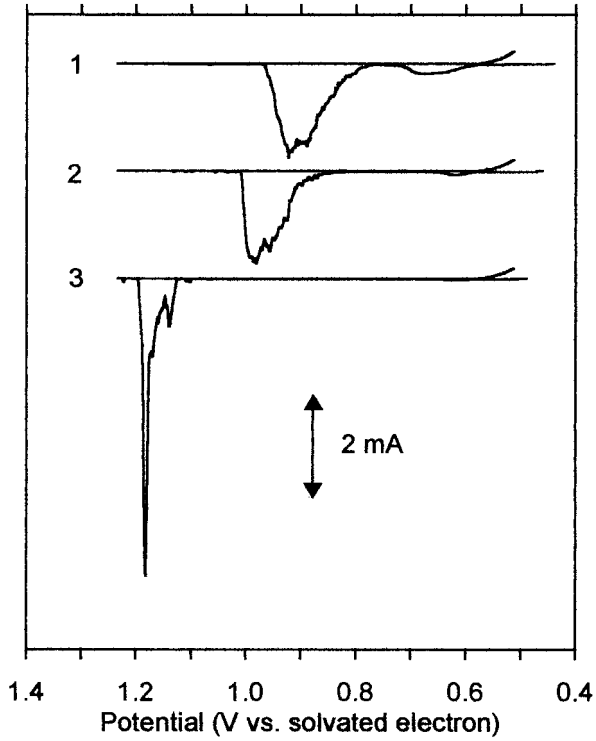


**Figure 11.** Voltammograms recorded for a 1 mm Pb disk in 1.0 M KI at − 70 °C after 40 s reduction at 0.274 V and different delay times at the open circuit potential. Delay time (s): 43 (1), 120 (2), 592 (3).

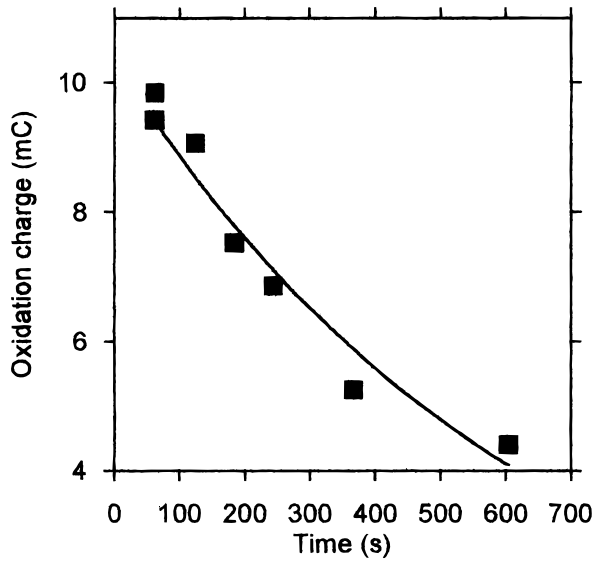


**Figure 12.** Oxidation charge of the deposit s3 plotted versus the delay time between the potentiostatic reduction and voltammetric oxidation of a 1 mm Pb disk in 0.1 M RbBr at −70 °C.

## Discussion

The principal processes occurring at low cathodic overpotentials or during the initial stages of lead reduction at high overpotentials are $Pb_9^{4-}$ generation as well as underpotential deposition (UPD) of the alkali metal. Similarly to other systems,[4,11a,k] the alkali metal UPD on lead is believed to be a preliminary step in a surface alloying. A fraction of the adsorbed alkali metal diffuses into lead, eventually to form intermetallic compound. However, both the surface coverage and the alkali metal concentration in the solid solution are likely to be diminished by the lead dissolution reaction. Therefore, crystalline intermetallic compounds are formed at relatively higher current densities than those that would be observed in the absence of the lead dissolution. Initially, the alkali metal-rich compound s2 is formed, but it is easily converted to the lead-rich compound via the reaction with the bulk lead. Similar reactions for the lithium/lead intermetallic compounds were reported by Kiseleva et al.[9] and for Cu/Cd alloys by Stevanovic et al.[36] When a compact layer of the lead-rich compound s3 is formed, diffusion of the alkali metal (and lead) through the compound layer starts controlling the overall rate of the reaction as well as its product distribution.

The growth of the solid layer as well as Zintl ion formation is strongly coupled and depends to a significant extent on the rate at which the alkali metal can be incorporated in lead. When the electrode is covered with the intermetallic compounds, the predominant electrochemical reaction is the incorporation of the alkali metal. This reaction can produce transitionally the alkali metal-rich compound s2 on the surface of s3:

$$Pb_{x1}M_{y1}(s3) + qe^- + qM^+ \Rightarrow Pb_{x1}M_{(y1+q)}(s2) \qquad (7)$$

$Pb_9^{4-}$, on the other hand, cannot be formed as a result of a simple reduction process, since the lead surface is covered with s2 and s3, in which the lead oxidation state is more negative than that in the Zintl ion. If $Pb_9^{4-}$ was produced by an electrochemical oxidation reaction of the deposit s2 or s3, its charge would strongly decrease on increasing the cathodic overvoltage, which was not observed. Therefore, the most likely reaction that produces $Pb_9^{4-}$ is an oxidative reduction, in which the lead-rich compound s3 produces both stronger reduced species s2 as well as $Pb_9^{4-}$ with a less negative oxidation state for lead:

$$Pb_{x1}M_{y1}(s3) + ze^- \Rightarrow Pb_{(x1-9z/4)}M_{y1}(s2) + (z/4)Pb_9^{4-} \quad (8)$$

The rate of this reaction is expected to increase exponentially with the cathodic overpotential. However, its occurrence will lower the surface activity of the substrate s3, which will lead to a rate decrease. Therefore, the net rate of the cathodic reaction will be limited, at least partially, by the rate at which s2 can be removed from the surface. The compound s2 cannot be oxidized electrochemically at cathodic overvoltages, but it can react with lead in a multistep process involving dissociation of s2, diffusion of the excess alkali metal through the s3 layer, and reaction with lead to form s3. Consequently, only a small increase in the $Pb_9^{4-}$ generation rate with the cathodic overpotential is observed.

Similar processes most likely take place during the s3 dissolution at the open circuit potential. In this case, however, the reaction shown in eq 8 is coupled to an oxidation reaction, since there is no current flow at the open circuit potential. As indicated by the open circuit potential experiments, the anodic reaction is the oxidation of the s2 deposit to form lead II. Simple stoichiometric calculations reveal that the zero current would result if only a part of the s2 present underwent oxidation. Therefore, the remaining part of s2 must react with bulk lead since there is no accumulation of s2 on the surface. The following two reactions fulfill the above requirements:

$$[(y1 - z)/y1]Pb_{(x1-9z/4)}M_{y1}(s2) + [9z(y1 - z)/4y1]Pb \Rightarrow [(y1 - z)/y1]Pb_{x1}M_{y1}(s3) \quad (9)$$

$$(z/y1)Pb_{(x1-9z/4)}M_{y1}(s2) \Rightarrow [z(x1 - 9z/4)/y1]Pb + zM^+ + ze^- \quad (10)$$

The sum of eqs 8−10, after rearrangement and simplification, corresponds to the s3 dissolution reaction at the open circuit potential:

$$(1/y1)Pb_{x1}M_{y1}(s3) + (9/4 - x1/y1)Pb \Rightarrow M^+ + (1/4)Pb_9^{4-} \quad (11)$$

In this case determination of the rate-limiting step of the dissolution was not possible. The dissolution rate is approximately 10 times slower than the rate of $Pb_9^{4-}$ generation at high cathodic overpotentials, which might suggest that the rate-limiting steps for dissolution are the electrochemical reactions 8 and 10. We note, however, that chemical reaction 9, even though in principle it is potential independent, becomes potential dependent under conditions of the electrochemical experiment due to coupling to the electrochemical processes 8 and 10. As mentioned earlier, this reaction is most likely diffusion controlled. The rate of diffusion is proportional to the alkali metal concentration gradient, which depends on the quantity of s2 on the surface. The quantity of s2 depends in turn on the rate of electrochemical processes 8 and 10.

The dependence of the stoichiometry of the lead-rich phase (s3) on the anodic scan rate and the reduction time when the potentiostatic reduction was followed immediately by voltammetric oxidation most likely reflects a nonequilibrium or non-steady-state distribution of the elements in the compound layer, e.g., presence of the alkali metal and lead diffusion profiles in the solid layer. These effects are definitely weaker after equilibration at the open circuit potential, where the reduction (and oxidation) currents are significantly lower. However, the stoichiometries determined under such conditions still reflect net compositions resulting from a simultaneous occurrence of many electrochemical and chemical reactions as suggested by the different stoichiometry of s3 in 1.0 and 0.1 M KI solutions. On the other hand, the Pb:M molar ratios do not depend on the equilibration (dissolution) time, since neither the dissolution rate nor the rest potential changes significantly with time. In other words, all the processes contributing to the dissolution occur at rates that do not change significantly with time and that give rise to a quasi-steady-state apparent stoichiometry.

As indicated by results of preparative electrolyses, phase s3 is not stable thermodynamically in the presence of lead and can react with it to form phases with a higher Pb content. This reaction, however, can occur only on electrodes, which were not activated electrochemically, since the phase s3 is then protected from dissolution by a passivating layer, most likely composed of lead carbonate or oxide. The electrochemical activation removes the protective layer which leads to much faster dissolution of s3 and thus prevents reaction between s3 and lead.

**Acknowledgment.** Financial support of the Welch Foundation is gratefully acknowledged.

## References and Notes

(1) Tomashova, N. N.; Kiseleva, I. G.; Astakhov, I. I.; Kabanov, B. N. *Elektrokhimiya* **1968**, *4*, 471.
(2) Teplitskaya, G. L.; Astakhov, I. I. *Elektrokhimiya* **1970**, *6*, 379.
(3) Teplitskaya, G. L.; Astakhov, I. I. *Elektrokhimiya* **1972**, *8*, 1199.
(4) Melendres, C. A. *J. Electrochem. Soc*. **1977**, *124*, 650.
(5) Kiseleva, I. G.; Alekseeva, L. A.; Teplitskaya, G. L.; Kabanov, B. N. *Elektrokhimiya* **1980**, *16*, 409.
(6) Alekseeva, L. A.; Kiseleva, I. G.; Kabanov, B. N. *Elektrokhimiya* **1980**, *16*, 413.
(7) Alekseeva, L. A.; Kabanov, B. N.; Kiseleva, I. G.; Popova, S. S. *Elektrokhimiya* **1982**, *18*, 1447.
(8) Baranski, A. S.; Fawcett, W. R. *J. Electrochem. Soc*. **1982**, *129*, 901.
(9) Kiseleva, I. G.; Tomashova, N. N.; Kabanov, B. N. *Elektrokhimiya* **1983**, *19*, 532.
(10) Astakhov, I. I.; Teplitskaya, G. L. *Elektrokhimiya* **1987**, *23*, 508.
(11) (a) Schultze, J. W.; Koppitz, F. D.; Lohrengel, M. M. *Ber. Bunsen-Ges.Phys. Chem*. **1974**, *78*, 693. (b) Kariv-Miller, E.; Nanjundiah, C. *J. Electroanal. Chem*. **1983**, *147*, 319. (c) Kariv-Miller, E.; Nanjundiah, C.; Eaton, J.; Swenson, K. E. *J. Electroanal. Chem*. **1984**, *167*, 141. (d) Kariv-Miller, E.; Svetlicic, V. *J. Electroanal. Chem*. **1985**, *205*, 319. (e) Kariv-Miller, E.; Lawin, P. B.; Vajtner, Z. *J. Electroanal. Chem*. **1985**, *195*, 435. (f) Garcia, E.; Cowley, A. H.; Bard, A. J. *J. Am. Chem. Soc*. **1986**, *108*, 6082. (g) Svetlicic, V.; Kariv-Miller, E. *J. Electroanal. Chem*. **1986**, *209*, 91. (h) Ryan, C. M.; Svetlicic, V.; Kariv-Miller, E. *J. Electroanal. Chem*. **1987**, *219*, 247. (i) Ryan, C. M.; Svetlicic, V.; Kariv-Miller, E. *J. Chem. Soc., Faraday Trans. 1* **1988**, *84*, 4023. (j) Lawin, P. B.; Svetlicic, V.; Kariv-Miller, E. *J. Electroanal. Chem.* **1989**, *258*, 357. (k) Aberdam, D.; Salem, C.; Durand, R.; Faure, R. *J. Electroanal. Chem.* **1990**, *239*, 71. (l) Svetlicic, V.; Lawin, P. B.; Kariv-Miller, E. *J. Electroanal. Chem*. **1990**, *284*, 185. (m) Fung, Y. S.; Lai, H. C. *J. Appl. Electrochem*. **1992**, *22*, 255. (n) Xie, G.; Ema, K.; Ito, Y.; Shou, Z. N. *J. Appl. Electrochem*. **1993**, *23*, 753. (o) Biallozor, S.; Lieder, M. *J. Electrochem. Soc*. **1993**, *140*, 2537. (p) Fidler, M. M.; Svetlicic, V.; Kariv-Miller, E. *J. Electroanal. Chem*. **1993**, *360*, 221. (q) Vaskevich, A.; Rosenblum, M.; Gileadi, E. *J. Electroanal. Chem.* **1995**, *383*, 167. (r) Radovic, B. S.; Edwards, R. A. H.; Jovicevic, J. N. *J. Electroanal. Chem.* **1997**, *428*, 113. (s) Kariv-Miller, E.; Lehman, G. K.; Svetlicic, V. *J. Electroanal. Chem.* **1997**, *431*, 87.
(12) Corbett, J. D. *Chem. Rev*. **1985**, *85*, 383.
(13) Zintl, E.; Dullenkopf, W. *Z. Phys. Chem. B* **1932**, *16*, 183.
(14) Zintl, E.; Harder, A. *Z. Phys. Chem. A* **1931**, *154*, 47.
(15) Kraus, C. A. *J. Am. Chem. Soc.* **1907**, *29*, 1557.
(16) Chlistunoff, J. B.; Lagowski, J. J. *J. Phys. Chem. B* **1997**, *101*, 2867.
(17) Lake, S. PhD Dissertation, University of Texas at Austin, Austin, 1998.
(18) Zintl, E.; Kaiser, H. *Z. Anorg. Allg.Chem*. **1933**, *211*, 113.
(19) (a) Pons, B. S.; Santure, D. J.; Taylor, R. C.; Rudolph, R. W. *Electrochim. Acta* **1981**, *26*, 365. (b) Eisenmann, B. *Angew. Chem., Int. Ed. Engl*. **1993**, *32*, 1693 and references therein. (c) Warren, C. J.; Ho, D. M.; Bocarsly, A. B. *J. Am. Chem. Soc*. **1993**, *115*, 6416. (d) Warren, C. J.; Ho, D. M.; Haushalter, R. C.; Bocarsly, A. B. *Angew. Chem., Int. Ed. Engl*. **1993**, *32*, 1646. (e) Warren, C. J.; Dhingra, S. S.; Ho, D. M.; Haushalter, R. C.; Bocarsly, A. B. *Inorg. Chem*. **1994**, *33*, 2709. (f) Warren, C. J.; Ho, D. M.; Haushalter, R. C.; Bocarsly, A. B. *Chem. Mater*. **1994**, *6*, 780. (g) Warren, C. J.; Haushalter, R. C.; Bocarsly, A. B. *J. Alloys Compd.* **1995,** *229*, 175.
(20) (a) Okada, M.; Guidotti, R. A.; Corbett, J. D. *Inorg. Chem*. **1968**, *7*, 2118. (b) Belin, C. H. E.; Corbett, J. D.; Cisar, A. *J. Am. Chem. Soc*. **1977**, *99*, 7163. (c) Edwards, P. A.; Corbett, J. D. *Inorg. Chem*. **1977**, *16*, 903. (d) Rudolph, R. W.; Wilson, W. L. *J. Am. Chem. Soc*. **1981**, *103*, 2480. (e) Critchlow, S. C.; Corbett, J. D. *Inorg. Chem*. **1982**, *21*, 3286. (f) Critchlow, S. C.; Corbett, J. D. *J. Am. Chem. Soc*. **1983**, *105*, 5715. (g) Burns, R. C.; Corbett, J. D. *Inorg. Chem*. **1985**, *24*, 1489. (h) Wilson, W. L.; Rudolph, R. W.; Lohr, L. L.; Taylor, R. C.; Pyykko, P. *Inorg. Chem*. **1986**, *25*, 1535. (i) Dhingra, S. S.; Haushalter, R. C. *J. Am. Chem. Soc*. **1994**, *116*, 3651.
(21) Chlistunoff, J. B.; Lagowski, J. J., unpublished results.
(22) Kolb, D. M. In Gerisher, H., Tobias, C. W., Eds. *Advances in Electrochemistry and Electrochemical Engineering*; Wiley: New York, 1978; Vol. 11, p 125 and references therein.
(23) Leiva, E. *Electrochim. Acta* **1996**, *41*, 2185 and references therein.
(24) Tindall, G. W.; Bruckenstein, S. *Electrochim. Acta* **1971**, *16*, 245.
(25) Vaskevich, A.; Rosenblum, M.; Gileadi, E. *J. Electroanal. Chem.* **1996**, *412*, 117.
(26) Chlistunoff, J. B.; Lagowski, J. J. Manuscript in preparation.
(27) Oldham, K. B.; Raleigh, D. O. *J. Electrochem. Soc*. **1971**, *118*, 252.
(28) James, S. D. *Electrochim. Acta* **1976**, *21*, 157.
(29) Lantelme, F. *J. Electroanal. Chem.* **1985**, *196*, 227.
(30) Epelboin, I.; Froment, M.; Garreau, M.; Thevenin, J.; Warin, D. *J. Electrochem. Soc*. **1980**, *127*, 2100.
(31) Gunawerdena, G.; Hills, G.; Montenegro, I.; Scharifker, B. *J. Electroanal. Chem.* **1982**, *138*, 225.
(32) Astakhov, I. I. *Elektrokhimiya* **1973**, *9*, 521.
(33) Wen, C. J.; Boukamp, B. A.; Huggins, R. A.; Weppner, W. *J. Electrochem. Soc*. **1979**, *126*, 2258.
(34) Lantelme, F.; Chelma, M. *J. Electroanal. Chem.* **1995**, *396*, 203.
(35) Elkhatabi, F.; Sarret, M.; Muller, C. *J. Electroanal. Chem.* **1996**, *404*, 45.
(36) Stevanovic, J. S.; Jovic, V. D.; Despic, A. R. *J. Electroanal. Chem*. **1993**, *349*, 365.